NASA Technical Memorandum 86723

Airborne Astronomy Program
Medium Altitude Missions Branch
Preprint Series 32

Submillimeter Observations of OH and CH in M42

Paul J. Viscuso, Gordon J. Stacey,
Charles E. Fuller, Noel T. Kurtz,
and Martin Harwit

September 1985

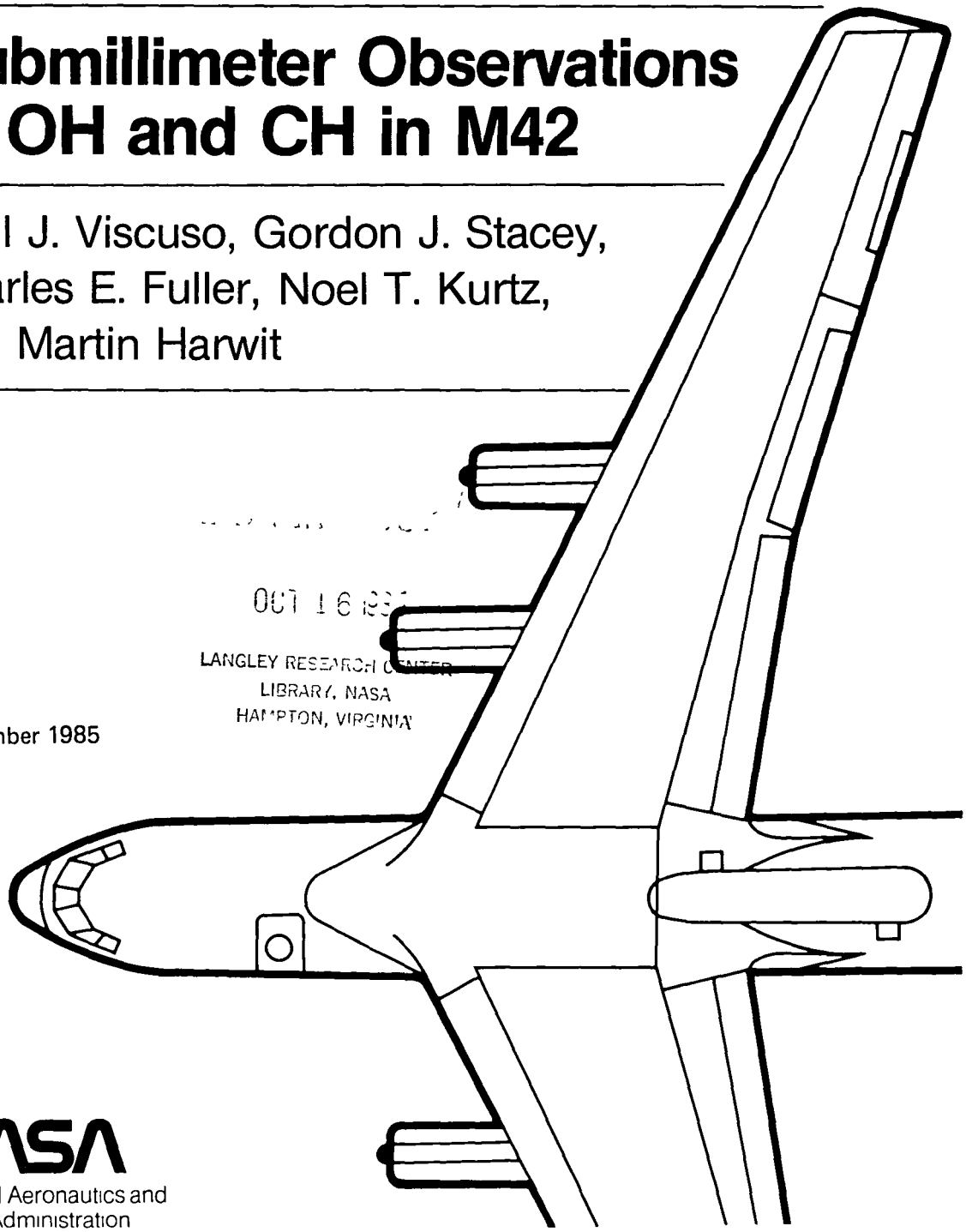

National Aeronautics and
Space Administration

NASA Technical Memorandum 86723

Airborne Astronomy Program
Medium Altitude Missions Branch
Preprint Series 32

Submillimeter Observations of OH and CH in M42

Paul J. Viscuso
Gordon J. Stacey
Charles E Fuller
Noel T Kurtz
Martin Harwit, Center for Radiophysics and Space Research, Cornell University, Ithaca, New York

September 1985

National Aeronautics and
Space Administration

Ames Research Center
Moffett Field California 94035

ABSTRACT

We have detected the $^2\Pi_{1/2}$(J = 3/2 to 1/2) transitions of OH at 163.12 and 163.40 μm, and obtained upper limits for the $^2\Pi_{3/2}$(J = 3/2 to 1/2) transitions of CH at 149.09 and 149.39 μm, in observations of the Kleinmann-Low Nebula of Orion. All four flux levels lie between 1 and 1.2×10^{-17} W cm^{-2}. The OH lines are bright when compared to the lower, $^2\Pi_{3/2}$(J = 5/2 to 3/2) fluxes reported by Storey et al. (1981) or Watson (1982) and imply that the 119 μm emission these authors observed is partially self-absorbed. The combined results provide strong constraints. Taken together with existing data on molecular hydrogen and CO (e.g., Scoville 1981, Shull and Beckwith 1982, Stacey et al. 1983) and recent data on other OH transitions (Viscuso et al. 1985)[1], they suggest OH emission from post-shock regions at temperatures T ~ 10^3 K, densities n_{H_2} ~ 7×10^6 cm^{-3} n_{OH} ~ 80 cm^{-3} optically thick for the $^2\Pi_{3/2}$ (J = 5/2 to 3/2), 119 μm but only partially self-absorbing in the (J = 7/2 to 3/2), 84 μm transitions over a Doppler velocity bandwidth of 30 km sec^{-1}. The OH column density is N_{OH} ~ 4×10^{16} cm^{-2} in the emitting regions which occupy a fraction g_f ~ 0.1 of a 1'×1' field of view centered on the Becklin-Neugebauer source. The CO (J = 31 to 30), 84 μm transition appears to lie sufficiently close to one of the 84 μm OH line components to be partially absorbed as well, through a Bowen-type mechanism.

[1]Viscuso, P. et al. , accepted for publication, Ap. J., 1985.

I. INTRODUCTION

During the past few years a number of interesting far-infrared and submillimeter spectral observations have shown excited CO and OH to be present in the Kleinmann-Low Nebula (K-L) of M42 (Watson et al. 1980, Storey et al. 1981, and Stacey et al. 1982). These observations are consistent with emission from a shocked or post-shock region which for CO has been found to have a temperature around 1000 K. For OH that temperature is not well established, but Watson (1982) assumes a temperature of 750 K. He argues for an OH column density $N_{OH} \sim 1.5 \times 10^{16}$ cm^{-2}, pointing out that such an amount of OH will lead to an optical depth for resonant scattering of $\tau \sim 40$ for an assumed line width of 30 km/sec. Recently, Matthews et al. (1985)[2] have reported emission in the Λ-doubling transitions within the rotationally excited state $^2\Pi_{3/2}$ ($J = 7/2$) with a broad (~25 km sec^{-1}) emission line-width in the $F = 4^+ \rightarrow 4^-$ component. Their observed flux is 10^{-25}W cm^{-2} or 10^{-2} photons cm^{-2} sec^{-1}, which contrasts with $\sim 5 \times 10^3$ photons cm^{-2} sec^{-1} per doublet component observed at 119 μm by Storey et al. and by Watson.

CH has, to date, not been reported in the Kleinmann-Low Nebula, though its abundance in the Galaxy is quite high in the general interstellar medium and though Rydbeck et al. (1976) observed CH emission in the ambient M42 complex, in regions that extended over 1 degree in diameter. Abundance estimates are difficult to make, but comparison to Goss's (1968) results suggested that CH/OH concentration ratios might be of the order of 0.2 for clouds of the class of M42. This is a very loose estimate, since the range could stretch a factor of

[2] Matthews, H. E., Baudry, A., Guilloteau, S., Winnberg, A., Submitted to A.&A., 1985.

3 higher or lower; but this ratio was high enough to encourage us to also search for CH in the Kleinmann Low-Nebula.

II. OBSERVATIONS

On the nights of March 14, 16, 17 and 21, 1983, we flew a series of four flights on the NASA Kuiper Airborne Observatory (KAO), during which we carried out a variety of observations on different celestial sources. Here, we will provide results obtained in observations on the Kleinmann-Low (K-L) region of M42, both for the OH transitions $^2\Pi_{1/2}$(J = 3/2 to 1/2) at 163.12 and 163.40 μm and for the $^2\Pi_{3/2}$(J = 3/2 to 1/2) transitions of CH at 149.09 and 149.39 μm. The wavelengths cited have been well established in laboratory studies, respectively by Brown et al. (1982) and by Brown and Evenson (1983).

We made use of our grating-interferometer instrument (Harwit et al. 1981), which provided us with a spectral bandpass of ~1.1μ and a resolution of 0.1 cm^{-1} corresponding to a resolving power of ~600 in the wavelength range of interest. The precision with which the wavelength corresponding to a given spectral bin could be determined was twice as high, 0.05 cm^{-1} corresponding to ~0.1 μm. Data on the OH lines were obtained on the nights of March 16 and 17. Data on CH were obtained on the nights of March 16, 17 and 21. Two sources of difficulty complicated the data reduction. The lines expected are weak, compared to the strong continuum radiation. In addition, there also is a strong CO transition (J = 16 to 15) at 162.812 μm, and strong telluric H_2O absorption at 148.7 μm. These additional features make for difficulty in establishing a baseline above which the OH and CH features have to be

discerned. Fig. 1 presents the OH data.

Confirming data were also obtained on flights carried out during the nights of January 26, 1984, and January 16, 1985, at an improved resolution of ~ 0.045 cm^{-1} corresponding to a resolving power of $\geq$1400 or a spectral discrimination of 0.023 cm^{-1} and a corresponding accuracy in wavelength determination of one part in ~ 3000.

Table 1 provides the line fluxes we determine. We feel that the OH lines are reasonably secure. The CH fluxes appear as weak indications which must be treated as upper limits and will have to be rechecked.

Table 1. Observed Fluxes due to OH and CH from M42

Wavelength	Molecule	Transition	Line Flux
163.12	OH	$^2\Pi_{1/2}$(J=3/2 to 1/2)	$1.2\pm0.6\times10^{-17}$ W cm^{-2}
163.40	OH		1.2 ± 0.6
149.09	CH	$^2\Pi_{3/2}$(J=3/2 to 1/2)	$\leq 1.0\pm1.0$
149.39	CH		$\leq 1.0\pm1.0$

The strengths of the lines listed in Table 1 were derived from the line-to-continuum ratio observed for the K-L region, using data of Werner et al. (1976) for the strength of the observed continuum radiation, assuming a 1', circular, continuum-emitting region. Since the main uncertainty in the signal strengths lies in the baseline subtraction, this is the factor which gives rise to the effective signal-to-noise ratios cited in Table 1. Far-infrared and submillimeter data currently available for OH and CH, both from other

groups and from ours, are summarized in Table 2. Figures 2 and 3 show the relevant energy level diagrams. These flux values are based on a calibration making use of continuum radiation levels in M42 established by Werner et al. (1976). Had we used corresponding values cited by Erickson et al. (1981), we would have obtained flux entries 30% higher throughout both tables.

Table 2. Data on OH and CH Transitions

Molecule	Transition	Excitation Temperature	Wavelength	Source	Transition Probability from Upper Levels* (sec^{-1})	Observed Flux Photons cm^{-2} sec^{-1}
OH	$(^2\Pi_{1/2})F_2 - F_2$ (J=3/2→1/2)	270 K	163.40 μm	This paper.	0.13†	10^4
			163.12		0.13	10^4
OH	$(^2\Pi_{3/2})F_1 - F_1$ (J=5/2→3/2)	120 K	119.44	Watson (1982).	0.14	4.8×10^3
			119.23		0.14	4.8×10^3
OH	$(^2\Pi_{3/2})F_1 - F_1$ (J=7/2→5/2)	290°K	84.60	Viscuso et al. (1985)	0.52	4.7×10^3
			84.42		0.52	3×10^3 ‡
OH	$(^2\Pi_{3/2})F_1$ (J=7/2)$4^+ \rightarrow 4^-$	290°K	2.2 cm	Matthews et al. (1985) (see footnote p. 3)	9.3×10^{-9}	10^{-2}
CH	$(^2\Pi_{3/2})F_2 - F_2$ (J=3/2→1/2)	95°K	149.39 μm	This paper.	0.034	$\leq 7 \times 10^3$
			149.09		0.034	$\leq 7 \times 10^3$
CH	$(^2\Pi_{1/2})F_1 - F_1$ (J=9/2→7/2)	390°K	88.55	Viscuso et al. (1985)	0.40	$<1.3 \times 10^3$

*From Destombes et al. (1977), Brown and Evenson, (1983), and Brown et al., (1982).

†This includes all downward transitions from the J=3/2 levels, not merely the 163μ transitions.

‡This includes the flux from the CO J = 31→30 transition at 84.411 μm (Viscuso et al. 1985).

III. QUANTITATIVE ANALYSIS

In this section we will attempt to tie together all the various data available to us on the radiating OH gas in the Kleinmann-Low region of M42. For that purpose we will make use of the infrared observations on line radiation, far-infrared continuum radiation observed in the same region, as well as near-infrared H_2 observations and radio data on CO (Scoville 1981) assumed to be coextensive with the observed OH. We start with a number of preliminary deductions which narrow down the possible ways in which these data can be juxtaposed.

Specifically, we will need to account for the following:

o The absolute as well as the relative line strengths of the different OH features that have been observed -- in particular the relatively low flux observed in the 119 μm lines compared to the flux observed at other wavelengths.

o The similarity of line strengths in the two OH components, respectively at 84.4 and 84.6 μm, observed by Viscuso et al., given the fact that the 84.4 μm component should appear considerably strengthened by an unresolved CO transition J = 31 to 30, only a Doppler shift of 30 km sec^{-1} removed from the OH component line center. That line strength can be determined from the strengths of neighboring CO features (e.g., Stacey et al. 1983).

o The strengths of highly excited CO transitions from states $J \geq 25$ cannot exceed observed values (Watson 1982), and that implies densities $n_{H_2} \leq 10^7$ cm^{-3} or temperatures $T \leq 750$ K for the OH-emitting region if it is coextensive with the CO-emitting gas.

o The observed Λ-doubling transitions within the $^2\Pi_{3/2}$ (J = 7/2)

state should be compatible with the 84 μm radiation emanating from this same level.

To that end, we adopt a number of assumptions:

i) Following the arguments of Stacey et al. (1982) we adopt a mass of 1.5 $M_\odot$, $N \sim 10^{57}$ molecules, for the post-shock hydrogen region at temperatures $\geq$ 750 K, and take a representative temperature to be 10^3 K.

ii) The 119 μm line observed by the Berkeley group (Storey et al. 1981, Watson 1982) and the 84 μm line observed by Viscuso et al. (1985) may be partially self-absorbed. That is far less likely for the 163 μm transitions, as we will see below. By referring the observed photon flux in these lines to a source at the distance of the Kleinmann-Low Nebula, we can infer that approximately 6×10^{47} photons per second emanate in the $^2\Pi_{1/2}$ lines alone.

iii) There are no spontaneous radiative transitions that go from the $^2\Pi_{3/2}$ ladder over to the $^2\Pi_{1/2}$ ladder (see Fig. 2), so the $^2\Pi_{1/2}$ transitions must be collisionally excited directly into that ladder. The collisional excitation cross sections to the individual parity states of that ladder have been measured by Andresen et al. (1984a, 1984b) for collision energies ~ 680 cm^{-1}, corresponding approximately to a temperature $T \sim 10^3$K. Most of the collisions into that ladder are followed by radiative deexcitation down the ladder, until the J = 3/2 state is reached. Summing over all the collisions that ultimately lead OH radicals to the $^2\Pi_{1/2}$ (J = 3/2) levels, we adopt an effective cross section ~ 2.2 $Å^2$ for the positive parity state and ~ 1.6 Å for the negative state. We can now set

$$N_\varepsilon \sigma_{coll} n_{OH} \delta v \sim 1.4\times10^{47}\varepsilon\, n_{OH} \sim 6\times10^{47}\ sec^{-1}$$

and therefore

$$n_{OH} \sim 4\,\varepsilon^{-1}\ cm^{-3}.$$

Here δv is the thermal velocity dispersion for molecular hydrogen, ~3.6 km sec^{-1} at $T = 10^3$ K, and n_{OH} is the density of OH radicals in the post-shock region. ϵ is the fraction of the post-shock gas containing OH.

iv) OH tends to be rapidly destroyed in shocks. When it does survive, it tends to be confined to a narrow region at some distance behind the shock and even there it retains low abundance. In the model of Draine and Roberge (1982) the OH is confined to a layer 5×10^{14} cm thick and reaches a maximum density amounting to only 1 percent of all the other forms in which oxygen occurs in the same region: O, H_2O, O_2, etc. Without tying ourselves to the particular model in other respects, we will adopt a layer thickness $d = 5\times10^{14}$ cm, and an abundance relative to atomic hydrogen of 6×10^{-6}.

$d = 5\times10^{14}$ cm

$n_{OH}/n_{H_2} \sim 12\times10^{-6}$ and therefore $n_{H_2} \sim 3.6\times10^{5}\ \epsilon^{-1}$ cm^{-3}

v) We will assume a large-scale velocity dispersion $\Delta v \sim 30$ km sec^{-1} for OH -- although, as above, we will assume a thermal velocity dispersion δv within any individual locale.

vi) We will adopt the collisional excitation cross sections of Andresen et al. (1984a, 1984b), shown also in Fig. 2. These lead to cross sections of ~ 2.5 $Å^2$, respectively, for direct excitation from the ground rotational state to the $^2\Pi_{3/2}$ ($J = 5/2^-$) state and to the $5/2^+$ state. Indirect excitation through collisions to higher states, followed by radiative transitions down to the 5/2 states, raise this cross section by roughly 30%.

vii) Finally, we will assume a filling factor, g_f, for the portion of our 1'×1' beam, from which OH is emitted. The value $g_f \leq 1/2$ is

suggested by the H_2 maps (e.g., Scoville 1981); but our angular resolution is far too small to rule out much smaller values of g_f indicating a small-scale clumpiness and knots of hot OH distributed on a far finer scale.

We now are in a position to derive some of the parameters that must characterize the emitting region and to describe the expected line flux:

a) The volume of the emitting regions V can be set equal to the total number of hydrogen molecules present, divided by the hydrogen density

$$V \sim \varepsilon \; N/n_{H_2}$$

In our 1' square field of view, at the distance of Orion, we encompass an area D^2, where $D = 4\times10^{17}$ cm. If the filling factor is g_f and the emitting layer has a thickness of $d = 5\times10^{14}$ cm, we obtain

$$V \sim D^2 \; d \; g_f = 8\times10^{49} \; g_f \; cm^3$$

$$n_{H_2} \sim \varepsilon \; N/V \sim 1.25\times10^{7} \; \varepsilon \; g_f^{-1} \; cm^{-3}$$

This estimate for n_{H_2} can be combined with that obtained under subsection (iv) above to yield

$$g_f \sim 35 \, \varepsilon^2$$

$$n_{H_2} \sim 2.1\times10^{6} \; g_f^{-1/2}, \; n_{OH} \sim 25 g_f^{-1/2}$$

Draine and Roberge as well as Chernoff et al. (1982) picture the Orion shock velocity to be ~ 35-40 km sec^{-1}, with a pre-shock density $n_{H_2} \sim 4\times10^{5}$ cm^{-3}. The post-shock density determined by pressure equilibrium would be $n_{H_2} \leq 8\times10^{7}$ cm^{-3}, for $T = 10^3$K, in the absence of magnetic fields, the density being highest at greater distances behind the shock. Hence $g_f \geq 10^{-3}$. We will anticipate a later result by

assuming g_f to be 0.1. Then $n_{H_2} \sim 6.6\times10^6$ cm^{-3}, $n_{OH} \sim 80$ cm^{-3}, $\varepsilon \sim 0.05$.

b) Collisional de-excitation occurs in a time

$$t_{cd} \sim [n_{H_2} \delta v \, \sigma_{cd}]^{-1} \sim 2340 \, (g_f/0.1)^{1/2} \text{ sec}$$

where we have set $\sigma_{cd} \sim 1.8\times10^{-16}$ cm^2, for the $^2\Pi_{3/2}$, J = 7/2 states. This is an estimate amounting to roughly twice the cross section for collisions leading to the ground, J = 3/2, state alone.

c) The density of 119 μm photons leaving the Nebula's surface in each doublet component n_ℓ (119 μm) is obtained directly from the observed flux F(119 μm) and the distance R of the Nebula

$$n_\ell (119\ \mu m) \sim F(119\ \mu m) \frac{2R^2}{D^2 g_f c} \sim 45 \, (g_f/0.1)^{-1}.$$

The flux due to the grain continuum radiation triples the number density at this wavelength, within the Doppler width Δv = 30 km sec^{-1}. Finally, if both the ingoing and outgoing components of the radiation are considered, in order to obtain an estimate of the actual number density of photons within the Doppler width of each line component, deep within the Nebula, we need to double the density once again. Within each of the two line components we therefore have an isotropic photon density deep inside the Nebula

$$n(119\ \mu m) \sim 270 \, (g_f/0.1)^{-1}.$$

d) The time duration over which an atom in the ground state can survive before absorbing a 119 μm photon is

$$t_a(119\ \mu m) \sim (n(119\ \mu m)\ c\ \sigma(119\ \mu m))^{-1} \sim 25(g_f/0.1) \text{ sec.}$$

Here we have made use of the absorption cross section calculated from the Einstein A-values given by Destombes et al. (1977), Table 2,

$$\sigma(\lambda_{ji}) = A_{ij} \frac{g_i}{g_j} \frac{\lambda_{ji}^3}{8\pi\Delta v}, \quad \sigma(119\ \mu m) \sim 5\times10^{-15}\ cm^2.$$

This estimate for t_a (119μm) may be high, if the grain-emitting region is not coextensive with the shocked domain. Collisional excitation out of the ground state, into any of the higher states shown in Fig. 2 occurs with a cumulative cross section $\sigma_{ce} \sim 13\ A^2$, and the time elapsed before ejection from this state through collisions becomes

$$t_{ce} \sim (\sigma_{ce}\ \delta v\ n_{H_2})^{-1} \sim 320\ (g_f/0.1)^{1/2}.$$

Collisional excitation into just one of the J = 5/2 parity states takes roughly five times longer. Between these two excitation rates, the time spent by an OH radical before excitation to the J = 5/2 state of the $^2\Pi_{3/2}$ ladder still is about $25(g_f/0.1)$ sec. Since the lifetime of that state before spontaneous emission is only 7 sec -- reduced to ~ 6 sec if stimulated emission is taken into account -- we see that the fraction of the population in the J = 5/2 state relative to that in the J = 3/2 state is

$$f(^2\Pi_{3/2},\ J = 5/2) \sim (5(g_f/0.1))^{-1}.$$

A similar analysis for the population of the $^2\Pi_{1/2}$ (J = 3/2) state yields t_a (53μm) = $710(g_f/0.1)^{-1}$, $t_{ce} \sim 1170(g_f/0.1)^{1/2}$ sec. Such a low value to t_a could explain all of the observed 163μm line radiation. The 84 and 119μm line emission, however, can only be explained through collisional excitation at a rate which also must produce approximately the observed 163μm line flux. This effectively sets an upper limit to the local 119μm photon density and also a lower limit to g_f.

e) About 45% of the collisional excitations lead from the ground state $^2\Pi_{3/2}$ (J = 3/2) into the $^2\Pi_{1/2}$ ladder, and about half of these

excited OH radicals eventually drop into the J = 1/2 state. The time spent in that state is determined by two factors, the radiative deexcitation time, ~ 27 sec, and the time elapsed before a 163 μm photon is absorbed, ~ 20 sec at the radiation density expected, but dependent on the particular hyperfine level in which the OH radical ends up. The fraction of the total population at any instant in the $^2\Pi_{1/2}$ (J = 1/2) state therefore is likely to be ~ 5 to 10%.

f) We now calculate the scattering optical depth at 84 μm, τ_s(84 μm). Making use of the absorption cross section for 84 μm radiation, σ(84 μm) ~ 6×10^{-15} cm^2, again obtained from the Einstein A-coefficient in Table 2, we have

$$\tau_s(84\ \mu m) \sim (n_{OH}\ f(^2\Pi_{3/2},\ J = 5/2)\ \sigma(84\ \mu m)\ d) \sim 48(g_f/0.1)^{-3/2}$$

To obtain the total number of resonant scattering events, τ_t, undergone before a photon can escape the shock, we make use of a result derived by Slater, Salpeter and Wasserman (1982), for $\tau_s \gg 1$,

$$\tau_t \sim 2\tau_s;\ \text{ then } \tau_t(84\ \mu m) \sim 96(g_f/0.1)^{-3/2}.$$

g) We still need to compute the absorption optical depth, given the number of resonant scattering events leading to escape from the Nebula. Since the lifetime against spontaneous emission from the $^2\Pi_{3/2}$ (J = 7/2) state is $(A(J = 7/2))^{-1}$ ~ 2 sec (Table 2), we see that the $96(g_f/0.1)^{-3/2}$ resonant scattering events mentioned above will cause OH molecules to spend a total of ~ $190(g_f/0.1)^{-3/2}$ sec in the J = 7/2 state. However, since we saw that state to be collisionally de-excited in $t_{cd} \sim 2340(g_f/0.1)^{1/2}$ sec, we conclude that the optical depth for absorption is

$$\tau_a(84\ \mu m) = \tau_t(84\ \mu m)\ (A(J = 7/2)\ t_{cd})^{-1} \sim 0.05(g_f/0.1)^{-2}.$$

The actual 84 μm optical depth could be somewhat higher, if our estimate

for the collisional deexcitation cross section is too low. A relatively small change in g_f could also raise the absorption.

h) At this point it is essential to note that the collisional excitation rates to the J = $7/2^+$ and $7/2^-$ states are in the ratio 1:1.5, according to Andresen et al. This ratio will therefore also be reflected in the strengths of the two 84 μm line-components and in the final populations of these two parity states. The 84.6 μm line should be stronger than the 84.4 μm component, but the nearby 84.4 μm CO transition may compensate, leading to rough equality.

If τ_a (84 μm) were as high as 0.3, we could have a partial but significant absorption not only of the two 84 μm OH transition but also of the CO, J = 31 to 30 rotational transition. The combined effect of these absorptions and of the larger collisional cross section giving rise to the 84.60 μm line could account for the apparent equal line strengths at 84.42 and 84.60 μm observed by Viscuso et al.

i) The scattering optical depth for the 119 μm radiation is substantially greater than that computed at 84 μm, primarily because more OH radicals will be in the ground state, even though the fraction of all OH radicals in that state is only $f(^2\Pi_{3/2}, J = 3/2) \sim 3/4$.

$$\tau_t(119\ \mu m) \sim 2\tau_s(119\ \mu m) \sim 2(n_{OH}\sigma(119\ \mu m) f(^2\Pi_{3/2}, J=3/2) d) \sim 300(g_f/0.1)^{1/2}$$

To compute the absorption optical depth we note that spontaneous emission from the $^2\Pi_{3/2}$ (J = 5/2) state occurs in $A(J = 5/2)^{-1} \sim 7$ sec, collisional de-excitation in $t_{cd} \sim 880(g_f/0.1)^{1/2}$ sec, since the collisional de-excitation cross section, again estimated as twice the cross section to the ground state alone, is ~ 4.9 Å^2, but that a third factor, namely stimulated emission, will also contribute roughly

with the same time constant as $t_a(119\ \mu m) \sim 25(g_f/0.1)$ sec. Hence

$$\tau_a(119\ \mu m) \sim \frac{\tau_t}{t_{cd}(A(J = 5/2) + (t_a(119\ \mu m)^{-1})} \sim 1.9(g_f/0.1)^{-1}.$$

We would therefore expect 119 μm photons to be reduced by about a factor ~ 6 or 7 through absorption, if $g_f = 0.1$. In fact, that was the prime reason for suggesting this value for g_f in section (a).

j) We can see that this g_f value must be roughly correct. Under (a), above, we had found a density $n_{H_2} \sim 2.1\times10^6 g_f^{-1/2}$ to give the observed 163 μm flux, provided this radiation was not self-absorbed. Since collisional excitation from the ground state , up the $^2\Pi_{3/2}$ ladder, is ~ 2 times as frequent as up the $^2\Pi_{1/2}$ ladder (Fig. 2), and since the 119 μm photon flux is only half the flux emitted from the $^2\Pi_{3/2}$ state, we see that the observed 119 μm flux will be obtained if only one-fourth of the 119 μm radiation emerges from the region unabsorbed. Hence, $g_f \sim 0.1$ in section (i). In addition, we already noted in subsection (d) above that a doubling of the 163 μm radiation could be achieved through absorption of 53 μm grain continuum emission. This may reduce the required self-absorption at 119 μm.

k) To account for roughly equal fluxes at 84 and 119 μm, we note that the collisional excitation rates to the $^2\Pi_{3/2}$ (J = 7/2) levels are about one-third the rates to the 5/2 level (Fig. 2). This lower excitation rate evidently compensates for the larger optical depth at 119 μm and keeps the 84 and 119 μm flux levels comparable.

l) The collisional excitation rates to the $^2\Pi_{1/2}$ (J = 3/2) and $^2\Pi_{3/2}$ (J = 7/2) levels are roughly comparable, but the significantly populated $^2\Pi_{1/2}$ (J = 5/2) states decay primarily through transitions

down the $^2\Pi_{1/2}$ ladder, almost doubling the number of transitions in the 163 μm line, as in Table 2.

m) We still need to take into account the relevant radio data. Matthews et al. (1985)[3] find a broad 13.44 GHz emission feature with a width of 25 km sec^{-1} in the $4^+ \rightarrow 4^-$ Λ-doubling transition of the $^2\Pi_{3/2}$ (J = 7/2) state. Though their field of view was 2.13', half-power width, it is most likely that this widened feature comes from the more confined shock-region. Their cited sensitivity 4.5 Jy K^{-1} and atenna temperature of 0.02 K corresponds to a 0.1 Jy flux over a 1.1 MHz bandwidth or 10^{-2} photons cm^{-2} sec^{-1} at the receiver. The Einstein A-coefficient for this transition is 9.3×10^{-9}, but stimulated emission by background photons dominates these radiative transitions, since

$$B(\nu) = \frac{\lambda^2}{8\pi} A(\nu) \sim 0.2\ A(\nu)$$

and the 3 K background radiation provides an effective photon flux from 4π sterad,

$$nc \sim 25\ cm^{-2}\ sec^{-1}$$

The transition rate, therefore, becomes

$$ncB(\nu) \sim 12.5A(\nu) \sim 10^{-7}\ sec^{-1}$$

for an OH radical in an excited $^2\Pi_{3/2}$ (J = 7/2), F = 4 state. Any additional background radiation would increase this stimulated emission. The ionized gas near the Kleinmann-Low Nebula could increase stimulated emission by an order of magnitude along our line of sight, if it were behind the Nebula. Since it is believed to be largely between the observer and the Nebula, however, it should not add to the stimulated emission. Some ionized gas on the far side of the Nebula can, however, not be entirely ruled out.

The region is optically thin to the 13.44 GHz radiation and we can

[3] Ibid p. 3

therefore compare this microwave flux to the 84 μm flux emanating from the same level. Matthews et al. observe only one polarization, and we recognize that their radiation comes only from one F level. With this in mind, and the 84 μm A-coefficient for this transition from Destombes et al., 5.3×10^{-1} sec^{-1}, we would expect, in our observations, to see

$$\leq 2\times10^{5} \text{ photons } sec^{-1} \text{ } cm^{-2}.$$

The fact that we see an order of magnitude less may be due both to stimulated emission at 13.44 GHz and to absorption at 84 μm.

n) Three predictions can be made, if the calculations outlined here are correct, and if the Andresen et al. (1984a, 1984b) collisional excitation cross sections prove to be accurate. First, we would expect the 163.4 μm line-component to be roughly 70% as strong as the 163.1 μm radiation in the flux received from the Kleinmann-Low Nebula. Second, we would expect the 119.2 μm flux to be ~ 13% weaker than the 119.4 μm flux. Both statements rest on cumulative collisional excitation rates up the $^2\Pi_{1/2}$ and $^2\Pi_{3/2}$ ladders, respectively. Third, the $^2\Pi_{1/2}$ (J = 1/2) state is likely to be appreciably populated, since it only decays slowly to the ground state. It should therefore resonantly scatter 163 μm radiation more effectively than the $^2\Pi_{3/2}$ (J = 3/2) state scatters 53 μm radiation. The 53 μm flux should, therefore, be stronger than expected solely on the basis of Einstein coefficients for the 53 and 163 μm transitions. Compared to the 163 μm line the 96 μm transition also should appear disproportionally strong.

These conclusions should be placed on a more secure basis through a multilevel radiative transfer computation which we expect to undertake.

IV. THE CH EMISSION

We now turn to the CH emission for which we have only been able to determine an upper limit in the 149 μm lines, comparable to the flux actually measured in the two 119 μm components of OH. It is not clear at which density CH would survive in the wake of a shock. CH readily combines with atomic oxygen to form CO, and it may well be that our observations are consistent with that reaction. Rydbeck *et al.* would suggest that CH would normally be four times less abundant than OH in regions like the Orion Nebula, but the densities expected in shocked gases might deviate considerably from that figure.

V. CONCLUSIONS

We can account for the flux levels observed in the 163 μm lines of the OH radical reported here, as well as the flux levels at 119 μm (Storey *et al.* 1981, Watson 1982) and 84 μm (Viscuso *et al.* 1985) by postulating emission from a gas cloud at temperature $T \sim 10^3$ K, having thickness $d \sim 5\times10^{14}$ cm with density $n_{H_2} \sim 7\times10^6$ cm^{-3} and OH abundance $n_{OH}/n_{H_2} \sim 12\times10^{-6}$; the post-shock domain is taken to occupy a fraction $g_f \sim 0.1$ our 1×1' field of view centered on the Becklin-Neugebauer object in the Kleinmann-Low Nebula. The OH column density is $N_{OH} \sim 4\times10^{16}$ cm^{-2} in the emitting regions. Optical-depth effects play a major role in determining the relative strengths of the observed lines. In particular, the 119 μm line components are strongly self-absorbed, and the 84 μm lines may be sufficiently self-absorbed, to also partly absorb the J = 31 to 30, CO emission from the gas despite the high $\Delta v \sim 30$ km sec^{-1} velocity dispersion along the line of sight.

Observational upper limits have also been placed on the CH, 149 μm flux from the same Nebula.

ACKNOWLEDGEMENTS

We would especially like to thank Dr. Kenneth Evenson of the National Bureau of Standards in Boulder for providing us with precise CH transition frequencies, prior to publication. Dr. Gary Melnick of the Smithsonian Institution's Center for Astrophysics was kind enough to help us in preparation for and during an early set of flights. Especial thanks are due to Drs. David Chernoff and Malcolm Walmsley who made several invaluable comments in extensive discussions on this topic, and suggested important changes. Dr. D. R. Flower sent us an informative private communication, Dr. Edward L. Wright was kind enough to point out a serious error in an earlier version of this paper and Dr. Dan Watson also provided a number of suggestions which we acknowledge with our thanks. We thank Drs. H. E. Matthews and H. W. Lülf for permitting us to make use of unpublished material of their respective groups; it led to considerable clarification of our interpretation of the data. We also would like to thank the personnel of the NASA-Ames Research Center for their cheerful and able support on our flights. The work was supported by NASA grant NSG 2347.

REFERENCES

Andresen, P., Häusler, D. and Lülf, H. W. 1984a, J. Chem. Phys., 81, 571.

Andresen, P., Häusler, D., Lülf, H. W. and Kegel, W. H. 1984b, A. + A., 138, L17.

Brown, J. M. and Evenson, K. M. 1983, Ap. J. Lett., 268, L51.

Brown, J. M., Schubert, J. E., Evenson, K. M. and Radford, H. E. 1982, Ap. J., 258, 899.

Chernoff, D. F., Hollenback, D. J. and McKee, C. F. 1982, Ap. J. Lett., 259, L97.

Destombes, J. L., Marliere, C., Baudry, A. and Brillet, J. 1977, Astron. Astrophys., 60, 55.

Draine, B. T. and Roberge, W. G. 1982, Ap. J. Lett., 259, L91.

Erickson, E. F., Knacke, R. F., Tokunaga, A. T. and Haas, M. R. 1981, Ap. J., 245, 148.

Goss, W. M. 1968, Ap. J. Suppl., 15, 131.

Harwit, M., Kurtz, N. T., Russell, R. W. and Smyers, S. 1981, App. Opt. 20, 3792.

Rydbeck, O. E. H., Koffberg, E., Hjalmarson, Å, Sume, A., Elldér, J. and Irvine, W. M., 1976, Ap. J. Supplement, 31, 333.

Scoville, N. Z. 1981, in Infrared Astronomy, I.A.U. Symposium #96, C. G. Wynn-Williams and D. P. Cruikshank, eds., p. 187.

Shull, J. M. and Beckwith, S. 1982, Ann. Rev. Astron. & Astrophys., 20, 163 (1982).

Slater, G., Salpeter, E. E. and Wasserman, I. 1982, Ap. J., 255, 293.

Stacey, G., Kurtz, N., Smyers, S., Russell, R., Harwit, M. and Melnick, G. 1982, Ap. J. Lett., 257, L37.

Stacey, G., Kurtz, N., Smyers, S. and Harwit, M. 1983, M.N.R.A.S., 202, 25P.

Storey, J. W. V., Watson, D. M. and Townes, C. H. 1981, Ap. J. Lett., 244, L27.

Watson, D. M. 1982, University of California, Physics Department Thesis, "Shock Waves and Mass Outflow in the Orion Molecular Cloud: Observations of Far-Infrared Emission Lines of Carbon Monoxide, Hydroxyl, and Ammonia."

Watson, D. M., Storey, J. W. V., Townes, C. H., Haller, E. E. and Hansen, W. L. 1980, Ap. J. Lett., 239, L129.

Werner, M. W., Gatley, I., Harper, D. A., Becklin, E. E. Loewenstein, R. F., Telesco, C. M. and Thronson, H. A., Ap. J., 204, 420 (1976).

FIGURE CAPTIONS

Figure 1 - Corrected observational spectrum of the 163μ region. The spectrum includes a correction for a ringing contribution due to the strong CO rotation transition feature at 162.82μ previously found by Stacey et al. (1983). The two OH features are indicated. The spectral resolution -- the ability to separate two contiguous lines of equal brightness is given by the separation of two spectral bins, 0.26μ. The separation between bins is 0.13μ.

Figure 2 - The OH-level diagram adapted from Brown et al. (1982). Numbers in parentheses are collisional cross sections from the $^2\Pi 3/2$ (J = 3/2) level as given by Andresen et al. (1984a and 1984b) and Schinke and Andresen (1985).

Figure 3 - The CH-level diagram adapted from Brown and Evenson (1983).

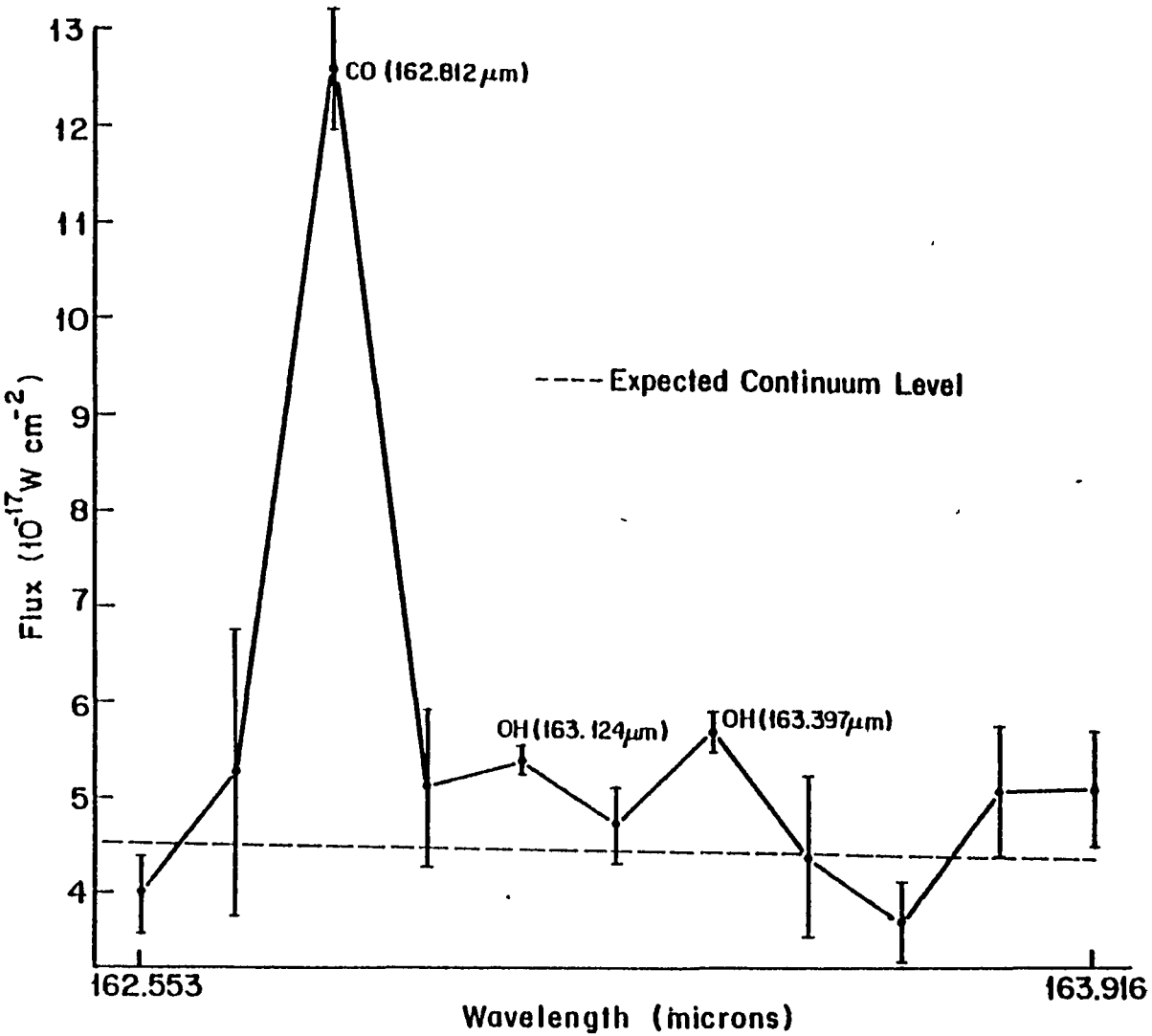
13
12
11
10
9
8
7
6
5
4
Flux (10^{-17} W cm^{-2})
CO (162.812 μm)
---- Expected Continuum Level
OH (163.124 μm)
OH (163.397 μm)
162.553
163.916
Wavelength (microns)

Figure 1

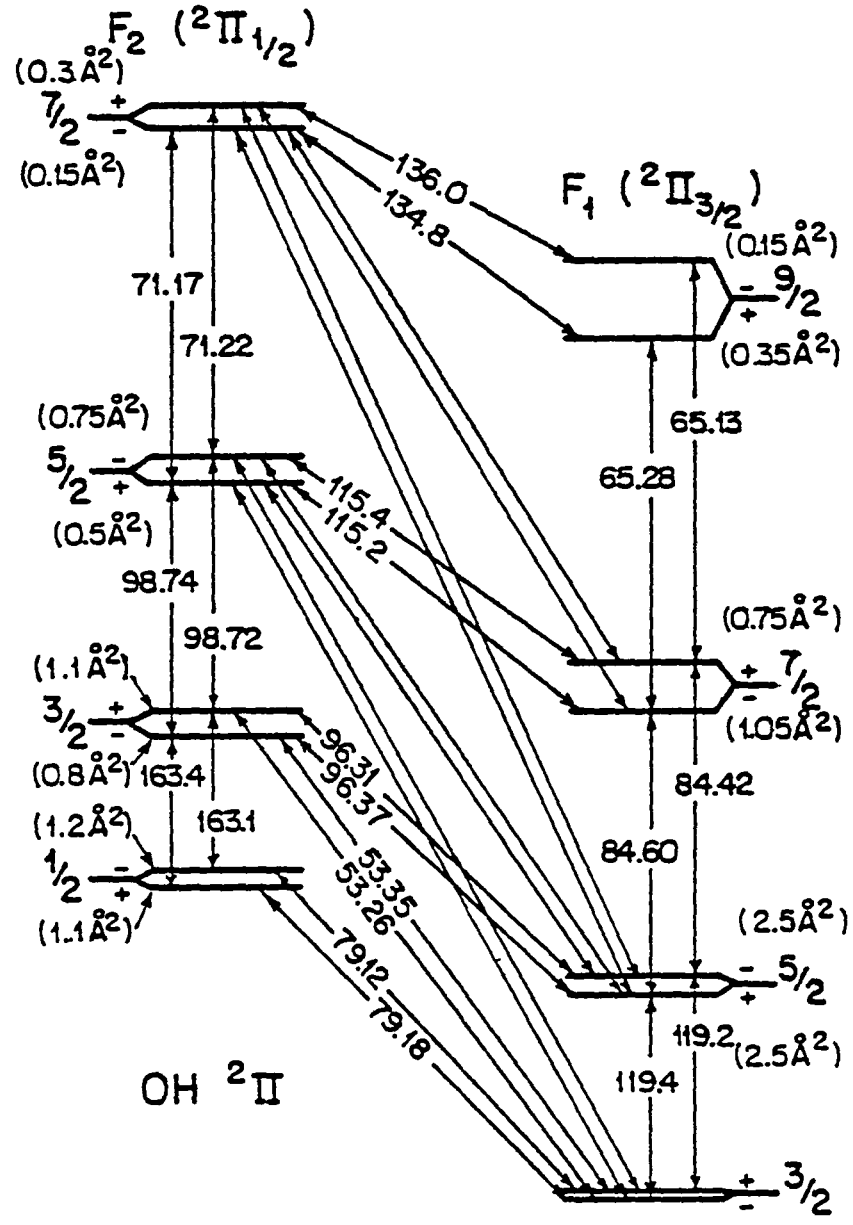
F2 (2Π1/2)
(0.3Å2)
7/2
(0.15Å2)
71.17
71.22
(0.75Å2)
5/2
(0.5Å2)
98.74
98.72
(1.1Å2)
3/2
(0.8Å2)
163.4
163.1
(1.2Å2)
1/2
(1.1Å2)
OH 2Π
136.0
134.8
115.4
115.2
96.31
96.37
53.35
53.26
79.12
79.18
F1 (2Π3/2)
(0.15Å2)
9/2
(0.35Å2)
65.13
65.28
(0.75Å2)
7/2
(1.05Å2)
84.42
84.60
(2.5Å2)
5/2
119.2
(2.5Å2)
119.4
3/2

Figure 2

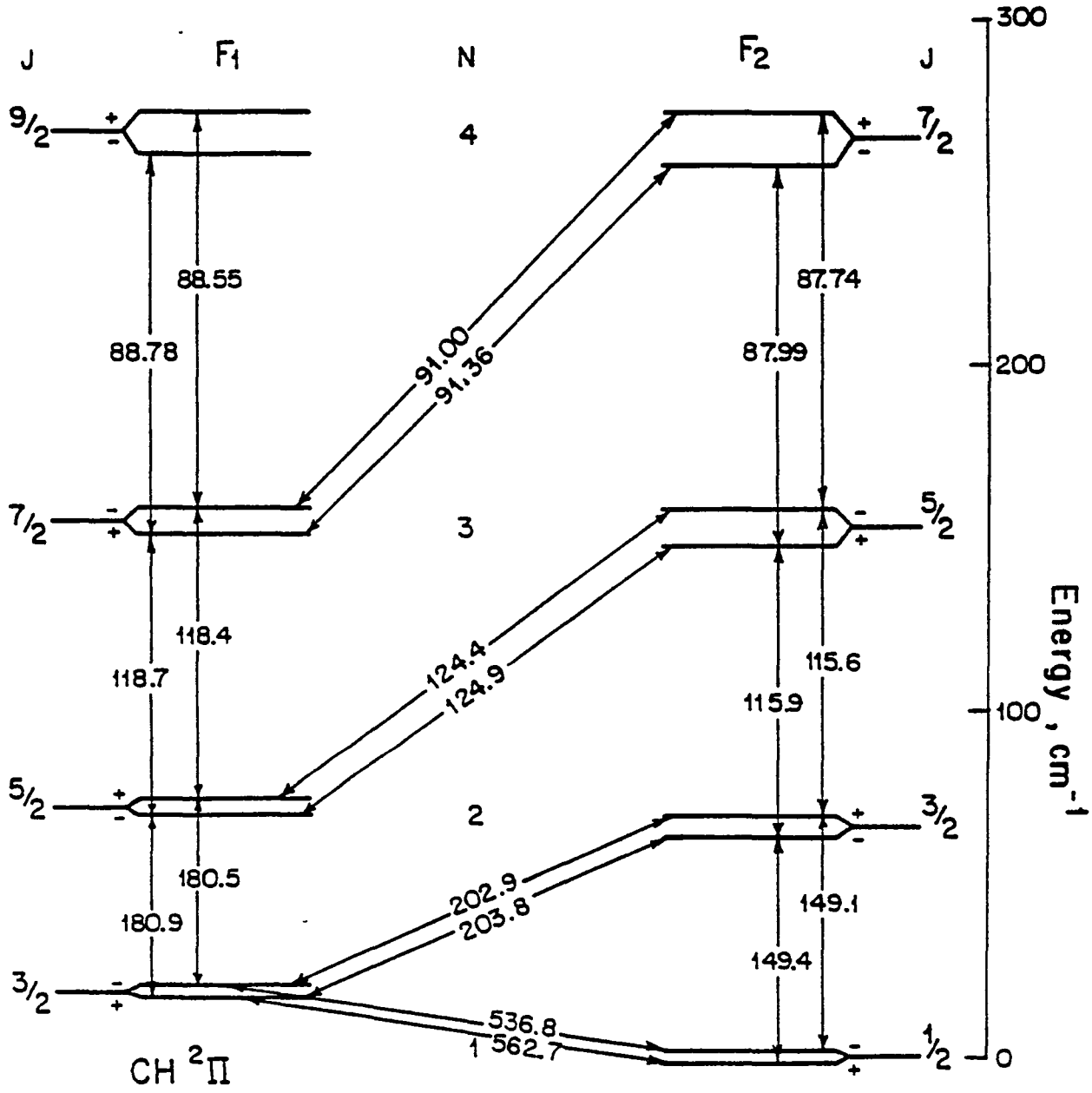
J
F1
N
F2
J
9/2
7/2
5/2
3/2
1/2
4
3
2
88.55
88.78
87.74
87.99
91.00
91.36
118.4
118.7
115.6
115.9
124.4
124.9
180.5
180.9
149.1
149.4
202.9
203.8
536.8
562.7
CH 2Π
300
200
100
0
Energy, cm-1

Figure 3

1 Report No	2 Government Accession No	3 Recipient's Catalog No
NASA TM-86723		

4 Title and Subtitle	5 Report Date
SUBMILLIMETER OBSERVATIONS OF OH AND CH IN M42	May 1985
	6 Performing Organization Code

7 Author(s)	8 Performing Organization Report No
Paul J. Viscuso, Gordon J. Stacy, Charles E. Fuller, Noel T. Kurtz and Martin Harwit	85224
	10 Work Unit No.

9 Performing Organization Name and Address	11 Contract or Grant No
Center for Radiophysics and Space Research, Cornell University, Ithaca NY 14853-0355	
	13 Type of Report and Period Covered

12 Sponsoring Agency Name and Address	13 Type of Report and Period Covered
National Aeronautics and Space Administration Washington, DC 20546	Technical Memorandum
	14 Sponsoring Agency Code 352-02-03

15 Supplementary Notes

Preprint Series #32. Supported by NASA grants.
Point of Contact: L. C. Haughney, Ames Research Center, M/S 211-12, Moffett Field, CA 94035 (415)694-5339 or FTS 464-5339

16 Abstract

We have detected the $^2\Pi_{1/2}$(J = 3/2 to 1/2) transitions of OH at 163.12 and 163.40 μm, and obtained upper limits for the $^2\Pi_{3/2}$(J = 3/2 to 1/2) transitions of CH at 149.09 and 149.39 μm, in observations of the Kleinmann-Low Nebula of Orion. All four flux levels lie between 1 and 1.2×10^{-17} W cm^{-2}. The OH lines are bright when compared to the lower, $^2\Pi_{3/2}$(J = 5/2 to 3/2) fluxes reported by Storey et al. (1981) or Watson (1982) and imply that the 119 μm emission these authors observed is partially self-absorbed. The combined results provide strong constraints. Taken together with existing data on molecular hydrogen and CO (e.g., Scoville 1981, Shull and Beckwith 1982, Stacey et al. 1983) and recent data on other OH transitions (Viscuso et al. 1985), they suggest OH emission from post-shock regions at temperatures $T \sim 10^3$ K, densities $n_{H_2} \sim 7 \times 10^6$ cm^{-3}, $n_{OH} \sim 80$ cm^{-3} optically thick for the $^2\Pi_{3/2}$(J = 5/2 to 3/2), 119 μm but only partially self-absorbing in the (J = 7/2 to 3/2), 84 μm transitions over a Doppler velocity bandwidth of 30 km sec^{-1}. The OH column density is $N_{OH} \sim 4 \times 10^{16}$ cm^{-2} in the emitting regions which occupy a fraction $g_f \sim 0.1$ of a 1' × 1' field of view centered on the Becklin-Neugebauer source. The CO (J = 31 to 30), 84 μm transition appears to lie sufficiently close to one of the 84 μm OH line components to be partially absorbed as well, through a Bowen-type mechanism.

17 Key Words (Suggested by Author(s))	18 Distribution Statement
Interstellar medium: shocks, cooling Molecular transitions Submillimeter astronomical spectroscopy	Unlimited Subject category - 89

19 Security Classif (of this report)	20 Security Classif (of this page)	21 No of Pages	22 Price*
Unclassified	Unclassified	28	A03

*For sale by the National Technical Information Service, Springfield, Virginia 22161

End of Document